CONF-771029--191

# PLASMA DRIVING SYSTEM REQUIREMENTS FOR COMMERCIAL TOKAMAK FUSION REACTORS

J. N. Brooks, R. C. Kustom, W. M. Stacey, Jr.

MASTER

Prepared for

7th Symposium on
Engineering Problems of Fusion Research
Hyatt-Regency
Knoxville, TN
October 25-28, 1977





ARGONNE NATIONAL LABORATORY, ARGONNE, ILLINOIS

operated under contract W-31-109-Eng-38 for the
U. S. ENERGY RESEARCH AND DEVELOPMENT ADMINISTRATION

Paper for presentation at the *Seventh Symposium on ENGINEERING PROBLEMS OF FUSION RESEARCH*, Knoxville, Tennesee, October 25-28, 1977, and for publication in the *Proceedings (IEEE)*.

# PLASMA DRIVING SYSTEM REQUIREMENTS FOR COMMERCIAL TOKAMAK FUSION REACTORS*

J. N. Brooks, R. C. Kustom, W. M. Stacey, Jr.

Fusion Power Program
Argonne National Laboratory
Argonne, Illinois 60439



*Work supported by the U. S. Department of Energy.

# PLASMA DRIVING SYSTEM REQUIREMENTS FOR COMMERCIAL TOKAMAK FUSION REACTORS*

J. N. Brooks, R. C. Kustom, W. M. Stacey, Jr.†
Fusion Power Program
Argonne National Laboratory
Argonne, Illinois 60439

## Introduction

The plasma driving system for a tokamak reactor is composed of an ohmic heating (OH) coil, equilibrium field (EF) coil, and their respective power supplies. Conceptual designs of an Experimental Power Reactor[1-3] (EPR) and scoping studies of a Demonstration Power Reactor[4] have shown that the driving system constitutes a significant part of the overall reactor cost. The capabilities of the driving system also set or help set important parameters of the burn cycle, such as the startup time, and the net power output. Previous detailed studies[1-3,5-6] on driving system dynamics have helped to define the required characteristics for fast-pulsed superconducting magnets, homopolar generators, and very high power (GVA) power supplies for an EPR.

The driving system requirements for commercial reactors have not been examined in detail to date. Plasma driving systems requirements are needed to guide studies of commercial reactor systems, to define research and development needs and to provide some perspective as to how well design options for near-term tokamaks extrapolate to commercial reactors. The plasma driving system requirements depend upon the reactor-design concept, of course. This paper summarizes our results[7] for a single reactor configuration together with several design concepts for the driving system. Both the reactor configuration and the driving system concepts are natural extensions from the EPR. Thus, the new results presented in this paper can be compared with the previous EPR results[1-3] to obtain a consistent picture of how the driving system requirements will evolve — for one particular design configuration.

## Reactor Model

The reactor model used for this study is an 8-m major radius tokamak having a plasma $\beta_t$ of about 8%, and a power output of 1000 MWe. The plasma is D-shaped with a height-to-width ratio of 1.3 and has equilibrium parameters $\bar{n}_{DT} = 1.44 \times 10^{20}$ m$^{-3}$, $I_p = 12.3$ MA, $q(a) = 3$, $\beta_p = 1.85$, $\bar{T}_{DT} = 8$ keV, and $\eta = 3\eta_{spitzer}$. The model and design parameters are based, in part, on data developed by the parametric systems analysis project at ANL.[8] The reactor coil configuration, shown in Fig. 1, is conventional, with a central, solenoidal OH coil with a few additional external trimming coils, and a set of EF coils external to the toroidal field coils. Both the OH and EF coils are superconducting and decoupled from one another. The locations of the EF coils and the relative currents in them have been selected so as to obtain the magnetic field in the plasma required to keep the plasma in MHD equilibrium. The peak field of the OH coils is 8 T. This and the OH coil radius of 3.3 m determine the available flux swing of the OH coil.

## Power Supply Configurations

Four different driving system power supply configurations have been examined as to their suitability for this reactor. Each configuration contains an energy transfer device for use with the OH coil during startup and a central energy storage device used to provide large power demands when necessary. Three types of possible OH transfer devices have been considered: (1) a homopolar generator; (2) an SCR-type rectifier-inverter power supply (SCR P.S.); and (3) a dump resistor. Two types of central energy storage devices have also been considered: (1) a *superconducting energy storage* inductor (ESI); and (2) a motor-generator-flywheel (MGF) set. These transfer and central storage devices have been combined into four configurations, the variable elements of which are listed in Table 1.

TABLE 1. Hardware Configurations

| Hardware Configuration No. | OH Transfer Device | Central Storage Storage Device |
|---|---|---|
| 1 | Homopolar generator | Energy storage inductor |
| 2 | SCR-type power supply | Energy storage inductor |
| 3 | SCR-type power supply | Motor-generator flywheel |
| 4a | Single dump resistor | Energy storage inductor |
| 4b | Multi-dump resistor | Energy storage inductor |

The equivalent circuit of Configurations 1 and 3 are shown in Figs. 2 and 3. All configurations use several common elements. The EF power supply is an SCR P.S. in all cases because the EF current cannot be free-running; it must be precisely controlled to keep the plasma in MHD equilibrium. (The MHD requirements depend on the plasma current and plasma pressure.) The requirements on the EF supply and the cost of it do, however, depend greatly on the type of OH transfer device used and upon details of the startup. The exact design of the EF supply also depends on whether it will operate out of an ESI or an MGF. All four configurations also use an auxiliary SCR P.S. in the OH circuit. This auxiliary supply is used to charge the OH coil prior to startup, and to make up for plasma resistance losses (supply volt-seconds) during the burn. Each configuration also involves a neutral beam power supply and a power supply that interfaces with the grid, power plant, and auxiliary subsystems. These have not been included in the cost estimates. The interfacing power supply is also used to recharge the central energy storage device. All of the configurations also incorporate a shorting switch (not shown) across the OH coil. This switch is opened just after the OH transfer device is connected, and is closed just before the transfer device is disconnected.

## Computational Model

The driving system requirements for this reactor have been analyzed by means of a spatial-profile-averaged, time-dependent, plasma code coupled to a driving system code. The plasma code solves particle balance equations for each constituent plasma ion species (D-T, alpha, wall-sputtered impurity) and solves energy balance equations for the ions and the electrons.

*Work supported by the U. S. Department of Energy.

†Present address: School of Nuclear Engineering, Georgia Institute of Technology, Atlanta, Georgia 30332.

Plasma heating by alpha and neutral beam slowing down is treated. Radiation (bremsstrahlung, line, recombination) and transport losses are treated, the latter with a multi-regime (neoclassical ions/empirical electrons at large collision frequencies and trapped-particle mode at small collision frequencies) confinement model. The overall model is described in Appendix C of Ref. 2. The inductance matrix for the poloidal coil system was computed on the basis of the coil locations shown in Fig. 1.[2] The inductance values are $L_p$ = 13.75 μH, $L_{OH}$ = 3.07 $N_{OH}^2$ μH, and $L_{EF}$ = 3.09 $N_{EF}^2$ μH, where $N_{OH}$ and $N_{EF}$ are the number of turns in the OH and EF coils respectively. The coefficients of coupling for the system are $K_{OH,p}$ = 0.47, $K_{EF,p}$ = 0.27, and $K_{EF,OH}$ = -0.01.

The focus of the analysis was on the startup phase of the burn cycle during which most of the driving system requirements are set. The nature of the startup is dependent on the OH transfer device. For each transfer device burn cycle simulations were performed for a range of ohmic heating ramp times, $\Delta t_{OH}$, and neutral beam turns on times, $t_{B_0}$. In general, values of $t_{B_0} = \Delta t_{OH}$ gave the best results and these are the cases discussed here.

## Startup Using Homopolar Generator

An example of the startup, using a homopolar generator, is shown in Fig. 4 for the typical case of $\Delta t_{OH} = t_{B_0}$ = 2 s. ($V_{OH}$ and $V_{EF}$ are the coil voltages, $I_p$ is the plasma current, etc.) The homopolar generator is connected to the previously charged OH coil at the start of the cycle, t = 0 and disconnected at t = 2 s. During this period the OH current increase serves to induce current in the plasma. Neutral beam heating is initiated at t = 2 s and terminated at about t = 8 s when the plasma reaches an ignited equilibrium. The EF current begins at zero at the start of the cycle, and rises in accordance with the needs of the MHD equilibrium, as determined by the plasma pressure and current. The requirements on the driving system are computed from these waveforms where, for example, the maximum value of $V_{OH}$ determines the maximum field change at the OH coil, $\dot{B}_{OH}$, and the homopolar generator storage capacity, $U_{OH}$, the amount of ohmic heating flux swing used for startup determines the maximum burn time, etc. The driving system requirements, for this case, are: $U_{OH}$ = 937 MJ, $\dot{B}_{OH}$ = 2.9 T/S, the maximum EF power requirement $P_{EF}$ = 2.1 GVA, the ESI storage requirement ≈9 GJ. Based on the OH flux swing used for startup, $\Delta\phi_{OH}$ = 121 V-s, a maximum burn time of 28 min would be possible.

Figure 5 shows the sensitivity of some of the requirements for Configuration 1 for a range of $\Delta t_{OH}$. Short reversal times reduce the flux swing $\Delta\phi_{OH}$ because the plasma is cool for a shorter time, thus $\Delta I_{OH}$ and hence $U_{OH} \sim I_{OH}^2$ are correspondingly low. $\dot{B}_{OH}$ and $P_{EF}$, however, scale as $\Delta t_{OH}^{-1}$ and so increase with short $\Delta t_{OH}$. Long reversal times increase $\Delta\phi_{OH}$ and $U_{OH}$. The resulting increase in $\Delta I_{OH}$ tends to make $\dot{B} \sim \Delta I_{OH}/\Delta t_{OH}$ become flat. For $\Delta t_{OH} \geq 3$, the maximum value of $V_{EF}$ occurs after the OH reversal, i.e. during beam heating, and so increasing $\Delta t_{OH}$ has no further effect on $P_{EF}$. Reversal times greater than 4 s produce unstable results in the sense that small changes in the initial OH current produce large changes in the plasma current. This is due to the large resistive losses encountered for long $\Delta t_{OH}$, which makes for a highly nonlinear interaction between plasma resistance, plasma current, and plasma temperature. Basically, very short reversal times impose power and $\dot{B}$ problems, while long reversal times impose volt-second problems.

## Startup Using Dump Resistor

The motivation of using a resistor as the OH transfer device is to enable use of the full potential OH flux swing by starting the OH current at its maximum (negative) value, i.e. corresponding to a field of $B_{OH}$ = -8T. This could potentially be done with a homopolar generator or a rectifier power supply, but then the cost of the transfer devices would be prohibitive, compared to the resistor. When the resistor is connected to the OH coil it forms an equivalent R-L circuit; the resistor dissipates magnetic energy as heat, and the current decays. Since only one polarity of the OH current can be used, the use of a dump resistor, by itself, is restricted to situations where enough flux is available in one direction to support startup.

Figure 6 shows a typical startup using a single dump resistor. This case has a resistor value adjusted to give $|V_{OH}|^{max}$ = 115 V/turn at t = 0. The OH current is started at -90 MA-turns, corresponding to $B_{OH}$ = -8 T. Both $V_{OH}$ and $I_{OH}$ show, to first order, the exponential decay characteristic of a conventional L-R circuit. By t = 1.5 s = $\Delta t_{OH}$, the proper amount of volt-seconds has been delivered. At this time, therefore, the resistor is removed from the circuit by closing a shorting switch, thereby reducing $V_{OH}$ to 0 and terminating the OH current decay. The resistor is then switched out and the auxiliary power supply switched in. The shorting switch is then opened completing the process. The shorting switch must handle a maximum current of 90 MA-turns and must isolate against a maximum voltage of 115 V/turn for a maximum reactive power capability of 10.3 GVA. The other features of the startup are similar to those for the other configurations except that $V_{EF}$ peaks at t = 0, when $V_{OH}$ is maximum. The maximum value of $V_{EF}$ is also more than for the other configurations. Another difference is that energy is dissipated in the resistor, a total of $\Delta U_{OH}$ = 8071 MJ for this case, instead of being returned to the OH coil. This is probably not significant, at least for long burn pulses, since it represents only 8 s worth of output from the reactor.

The advantage of the dump resistor is evident from Fig. 6; at the end of the startup $I_{OH}$ is much lower than for the other transfer devices. The OH coil can therefore swing through much more flux, nearly double that for the other devices. This gives a maximum burn time capability of 57 min, for this case. Thus, the major advantage of using a dump resistor is to achieve a much longer burn time for a given $B_{OH}^{max}$.

The sensitivity of some of the driving system requirements to the parameter $V_{OH}^{max}$, for Configuration 4a, is shown in Fig. 7. In this figure the lowest value of $|V_{OH}|^{max}$ shown is the lowest that works; lower values result in complete resistive current decay in the plasma.

## SCR Power Supply

A similar study was performed for the configurations using an SCR power supply as the OH transfer element. In general, the EF supply and the ESI have similar requirements to the homopolar generator cases. $\dot{B}_{OH}$ is somewhat lower if a flat $V_{OH}$ waveform is used. The requirement on the OH-SCR supply itself is about 2.0 GVA. The OH volt-second consumption during startup, and hence the maximum burn time, is similar to the homopolar generator cases.

## Power Supply Costs

Figure 8 summarizes the total driving system power supply cost as a function of the OH ramp time for the different configurations. This data has been generated by applying cost algorithms[7] developed for the various hardware components to the technological requirements found by the burn cycle analysis. This cost covers the Oh transfer device, the OH auxiliary supply, the EF supply, the central energy storage device, and all switch costs. (While the heating system costs are not included

the energy storage requirement on the central storage device due to the neutral beam is included. Figure 8 is for the case of the neutral beam turned on just after the OH ramp, generally the best operating mode. The cost of each configuration is extremely sensitive to the ramp time; this illustrates the need for a very precise and coupled analysis of the plasma and the driving system. In general, the cheapest operating point is the most cost effective.

Configuration 1 results in the smallest power supply cost: 105 \$M for a $\Delta t_{OH}$ of 3 s.

In Configuration 2, at the cheapest operating point, $\Delta t_{OH}$ = 2.3 s, the cost is about 30 \$M more than for Configuration 1. This is basically because the SCR supply costs more than the homopolar generator. The requirements for this case are $P_{OH}$ = 2.1 GVA, $P_{EF}$ = 1.6 GVA, $\dot{B}_{OH}$ = 2.0 T/s, and ESI storage = 8.4 GJ.

Configuration 3 is the most conventional in terms of available technology. MGF sets are presently used. The rectifier supply for the MGF system is a conventional ac-dc multiphase converter, rather than a dc-ac-dc inductor-converter of the type needed for use with the ESI. Although the requirements for this configuration, exclusive of the MGF set, are the same as for Configuration 2, the cost is much higher and nearly double that of the homopolar generator-ESI combination at the cheapest operating point. This large additional cost is due almost entirely to the cost of the generator portion of the MGF set. Furthermore, the cost estimates for this configuration assume a voltage compatible power supply-MGF-set combination, i.e. with no transformers used. If transformers were needed the cost of Configuration No. 3 would be even greater.

In Configuration 4a the use of a dump resistor, which has an essentially trivial cost, eliminates the need for a symmetric OH current swing during startup (needed for the other transfer devices), and so permits the full design value of the OH flux swing to be used. The potential burn time is, therefore, doubled, relative to the other transfer devices. The use of a dump resistor, however, requires a voltage isolating-shorting switch, in the OH circuit. If this switch must be solid state, as has been assumed, it will be expensive. For example, for the example described earlier of $|V_{OH}|^{max}$ = 115 V/turn, the switch cost is estimated to be 82 \$M whereas the cost of the resistor, at 0.6 \$M is negligible in comparison. Also, the range of ramp times, for a single dump resistor, is limited to fairly short times, and this increases the EF requirements. For these reasons, Configuration 4a is comparatively expensive, about 185 \$M for the cheapest case. This may or may not be worth the doubled burn time. Requirements for this case are $\dot{B}_{OH}$ = 3.4 T/s, $P_{EF}^{max}$ = 2.6 GVA. If four resistors are used, to obtain a variable resistance during startup, as in Configuration 4b, the maximum OH voltage during startup can be lowered and the ramp time increased. This saves on EF supply cost relative to Configuration 4a but involves higher switch costs. The cheapest case for Configuration 4b costs about the same as Configuration 4a. The burn time is the same, $\dot{B}_{OH}$ = 2.0 T/s and $P_{EF}^{max}$ = 1.6 GVA are lower, while circuit complexity and control would be greater.

## Conclusion

In general, feasible startup times for this typical commercial reactor are about the same as for an EPR; OH reversal times of 1-4 s followed by a beam heating period of about 5 s. The $\dot{B}$ requirements on the OH coil are considerably less than for an EPR, basically due to the larger radius of the OH coil. The OH power and energy requirements are similar to an EPR but the EF requirements increase considerably. In general, there is a strong degree of coupling between the driving system requirements and the details of the plasma physics, particularly the temperature behavior and the MHD field requirements of the plasma.

Naturally, the results described here are subject to uncertainties in the plasma physics and in the cost algorithms. However, the relative cost data between the different power supply technologies seems clear. Conventional technology, in the form of an MGF set and conventional SCR supply can be used for the driving system but the cost will be high. Development of superconducting energy storage systems and homopolar generators appear to offer very substantial savings; in the neighborhood of 100 \$M per reactor.

## References


1. W. M. Stacey, Jr., et al., "EPR-77: A Revised Design for the Tokamak Experimental Power Reactor," Argonne National Laboratory, ANL/FF/TM-77 (1977).
2. W. M. Stacey, Jr., et al., "Experimental Power Reactor Conceptual Design," Argonne National Laboratory, ANL/CTR-76-3 (1976).
3. W. M. Stacey, Jr., et al., "Tokamak Experimental Power Reactor Studies," Argonne National Laboratory, ANL/CTR-75-2 (1975).
4. D. Steiner, et al., "ORNL Fusion Power Demonstration Study: Interim Report," ORNL/TM-5813 (1977).
5. F. E. Mills, Ed., "Plasma Driving Systems for a Tokamak Experimental Power Reactor," in *Proc. 2nd ANS Top. Mtg. on Technology of Controlled Nuclear Fusion*, USERDA CONF-760935, Vol. IV, p. 1233.
6. J. N. Brooks and W. M. Stacey, Jr., "Driving Requirements for the Ohmic Heating and Equilibrium Coils of a Tokamak Experimental Power Reactor," in *Proc. 6th IEEE Symp. on Engineering Problems of Fusion Research*, IEEE Pub. No. 75CH1097-5-NPS, p. 43 (1975).
7. J. N. Brooks, et al., "Plasma Driving Systems Requirements for Commercial Tokamak Fusion Reactors," Argonne National Laboratory, ANL/FPP/TM-87 (1977).
8. M. Abdou, et al., "Parametric Systems Analysis for Tokamak Power Plants," Argonne National Laboratory, ANL/FPP/TM-97 (1977).

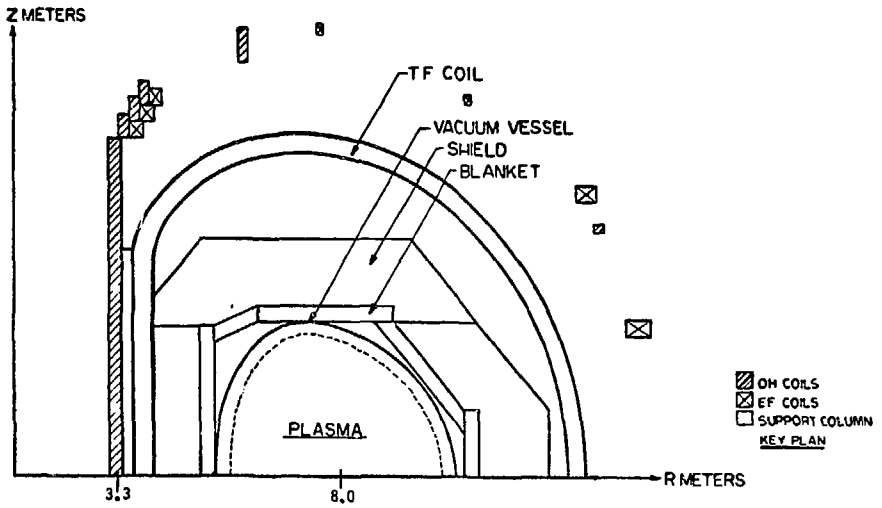


Fig. 1. Schematic view of OH and EF coil locations.

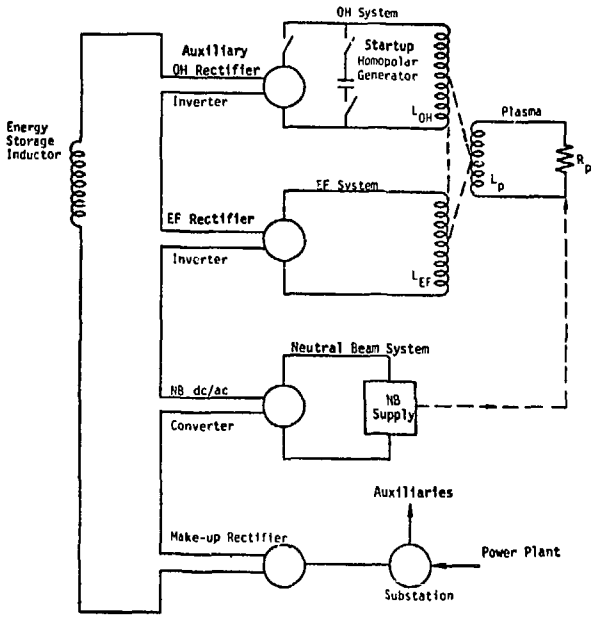


Fig. 2. Power supply Configuration 1.

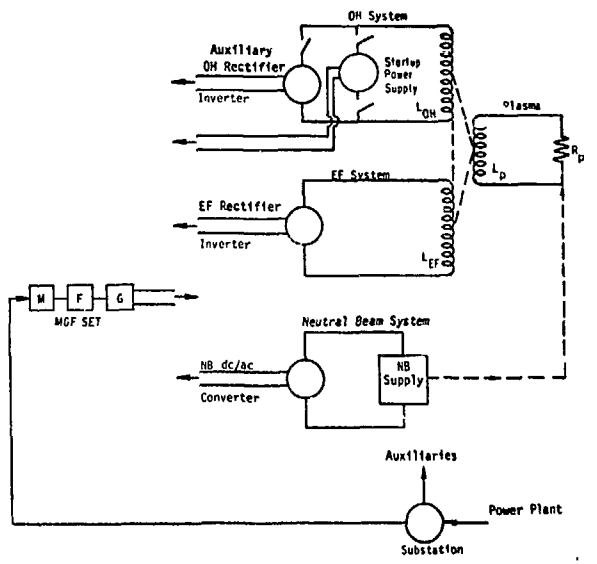


Fig. 3. Power supply Configuration 3.

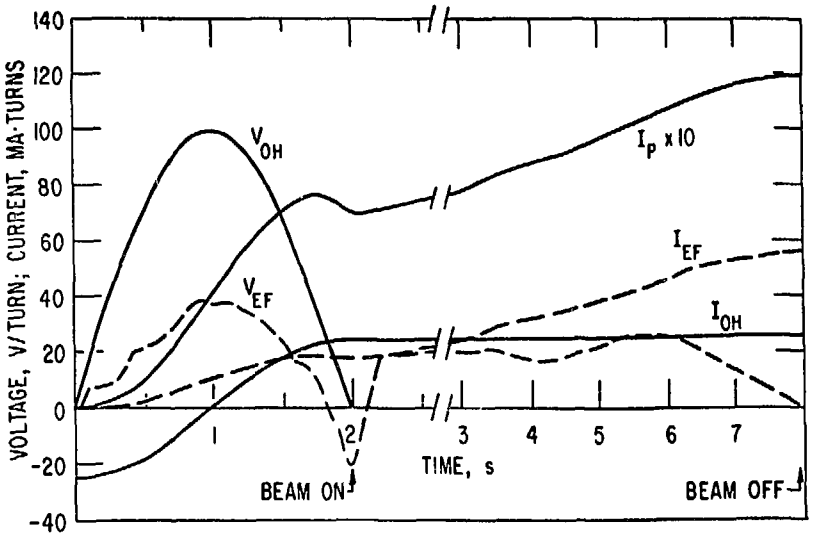


Fig. 4. Typical startup using a homopolar generator as the OH transfer element. $\Delta t_{OH}$ = 2 s, $t_{B_0}$ = 2 s.

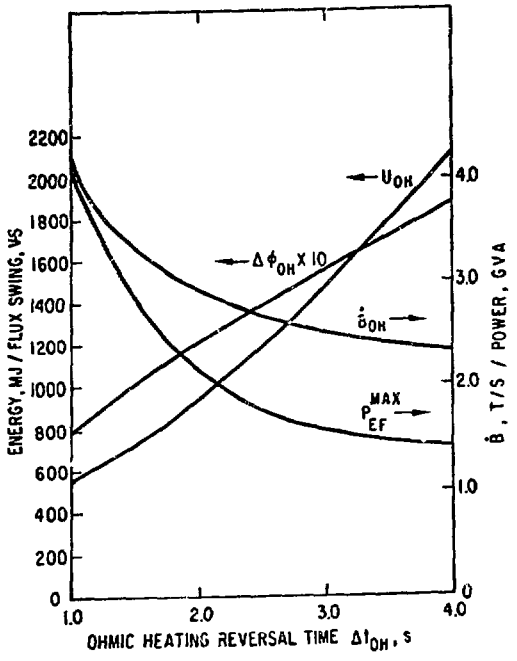


Fig. 5. Sensitivity of the driving system requirements to the ohmic heating ramp time, $\Delta t_{OH}$. For a homopolar generator used as the OH energy transfer device.

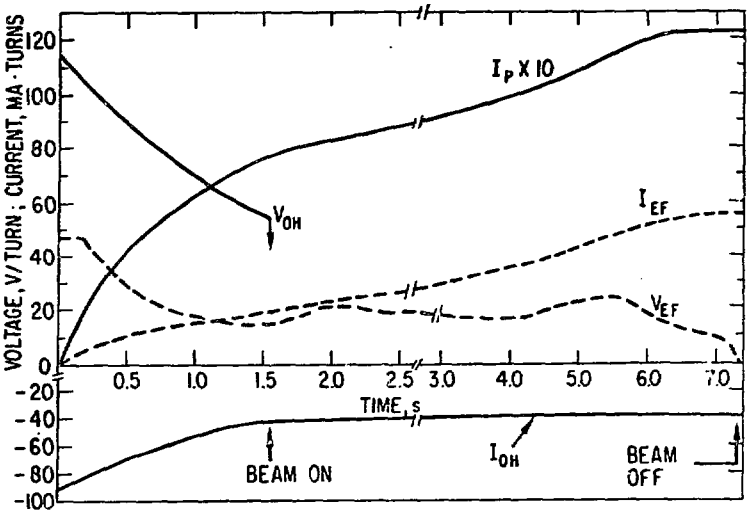


Fig. 6. Typical startup using a dump resistor as the OH transfer element; $V_{OH}^{max}$ = 115 V/turn, $t_{B_0} = \Delta t_{OH}$.

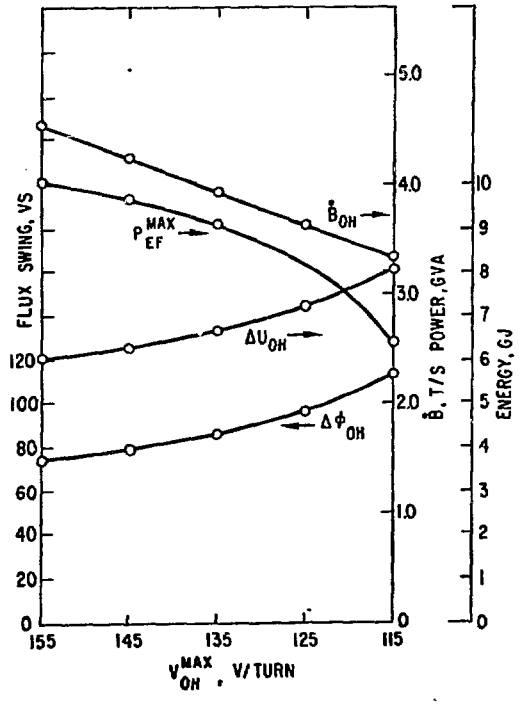


Fig. 7. Sensitivity of the driving system requirements to the maximum OH voltage. For a single dump resistor used as the OH transfer element.

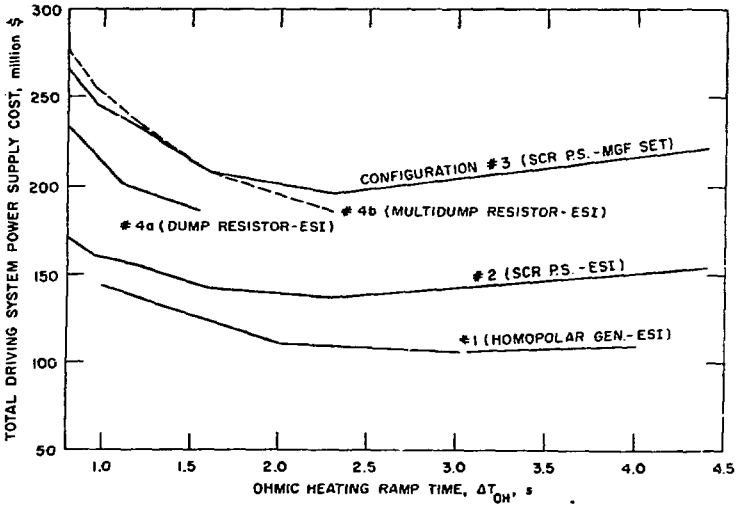


Fig. 8. Total driving system power supply cost as a function of the OH ramp time, $\Delta t_{OH}$ and power supply configuration. For the neutral beam turn-on time, $t_{B_0} = \Delta t_{OH}$